ISSN 1070-3284, Russian Journal of Coordination Chemistry, 2019, Vol. 45, No. 8, pp. 600–607. © Pleiades Publishing, Ltd., 2019.

Syntheses, Structures, and Properties of Two Cd(II)/Zn(II) Complexes with 1,2,4-Triazole Derivatives

F. Y. Ju[a], G. L. Li[b], X. L. Li[b], W. D. Yin[a], and G. Z. Liu[b, *]

[a]*School of Food and Drug, Luoyang Normal University, Luoyang, 471934 P.R. China*

[b]*College of Chemistry and Chemical Engineering and Henan Key Laboratory of Function-Oriented Porous Materials, Luoyang Normal University, Luoyang, 471934 P.R. China*

**e-mail: gzliuly@126.com*

Received June 25, 2018; revised October 24, 2018; accepted November 23, 2018

Abstract—Two new coordination polymers, $\{[Cd(Hmph)(Itmb)] \cdot H_2O\}_n$ (**I**) and $[Zn(Hmph)(Bpt)_2]_n$ (**II**) (H_2Hmph = homophthalic acid, Itmb = 1-(imidazo-1-yl)-4-(1,2,4-triazole-1-ylmethyl)benzene, Bpt = 3,5-bis(4-pyridyl)-1,2,4-triazole) have been prepared and then characterized by single crystal X-ray diffraction (CIF files CCDC nos. 1842595 (**I**), 1842591 (**II**)). Complex **I** shows a 2D layer structure containing Cd-carboxylate chains linked further by itmb coligands, and the ultimate 3D supramolecular structure is stacked through significant π–π interactions. Complex **II** displays a zigzag Zn-carboxylate chain structure, which is further extended to the final 3D supramolecular structure by hydrogen-bonding and π–π interactions. TGA experiments indicate that complex **I** and **II** have high thermal stabilities because they can maintain framework integrity until 275 and 315°C, respectively. And in comparison, with the free ligands, the fluorescent properties of both CPs show significant blue-shift.

Keywords: homophthalic acid, 1,2,4-triazole derivatives, thermal stabilities, fluorescent properties

DOI: 10.1134/S1070328419080049

INTRODUCTION

As is well known, coordination polymers (CPs) are a class of important hybrid materials realized by various metal ions and selected organic chemicals [1–5]. In this respect, the mixed-ligand strategy has been employed extensively and proved to be a reliable approach to design and construct expecting CPs with attractive structures and desirable applications [6–11]. Typically, the compounds based on bipyridyl groups featuring two 4-pyridyl or 2-pyridyl groups separated by different spacers are involved as nitrogen donor ligands, while aromatic or aliphatic multi-carboxylates with rigid or flexible backbones are used as the oxygen donor ligands [12–15]. And some novel N-donor ligands containing imidazolyl, triazolyl or tetrazolyl groups have been probed because the species of ligands have been unable to satisfy the need of sustainable growth of CPs chemistry [16–21]. The 1,2,4-triazole and its derivatives have attracted great attention for the reasons detailed as bellow: firstly, abundant nitrogen atoms of 1,2,4-triazole ring can provide three potential coordination sites and versatile coordination modes to meet or mediate the coordination requirements of different centre mental ions; secondly, even if one and more nitrogen atoms of 1,2,4-triazole ring can not participate in coordination, they are inherent good donors or acceptors for hydrogen atoms to establish hydrogen-bonding interactions. Therefore, the introduction of 1,2,4-triazole can impact intensively on the ultimate supramolecular structures and their potential functions.

Particularly, we selected elaborately two nitrogen donor ligands, namely 1-(imidazo-1-yl)-4-(1,2,4-triazole-1-ylmethyl)benzene (Itmb) and 3,5-bis(4-pyridyl)-1,2,4-triazole (Bpt). Except the triazolyl ring, there are imidazolyl and phenyl group for Itmb molecule, and two 4-pyridyl groups for Bpt molecule, which can provide more possible coordination sites and more opportunity to produce the non-covalent interactions such as hydrogen-bonding and π–π stacking interactions. Meanwhile, the strong steric hindrance in both nitrogen donor ligands can influence profoundly on the self-assemblies of CPs. To the best of our knowledge, there are few documents on CPs constructing from Itmb ligand and more reports about CPs based on Bpt ligand. As summarized in Scheme 1 (a–h), Itmb molecule can act as mono or bidentate ligand [22, 23], while Bpt molecule exhibits versatile coordination modes from monodentate to tetradentate [24–28].

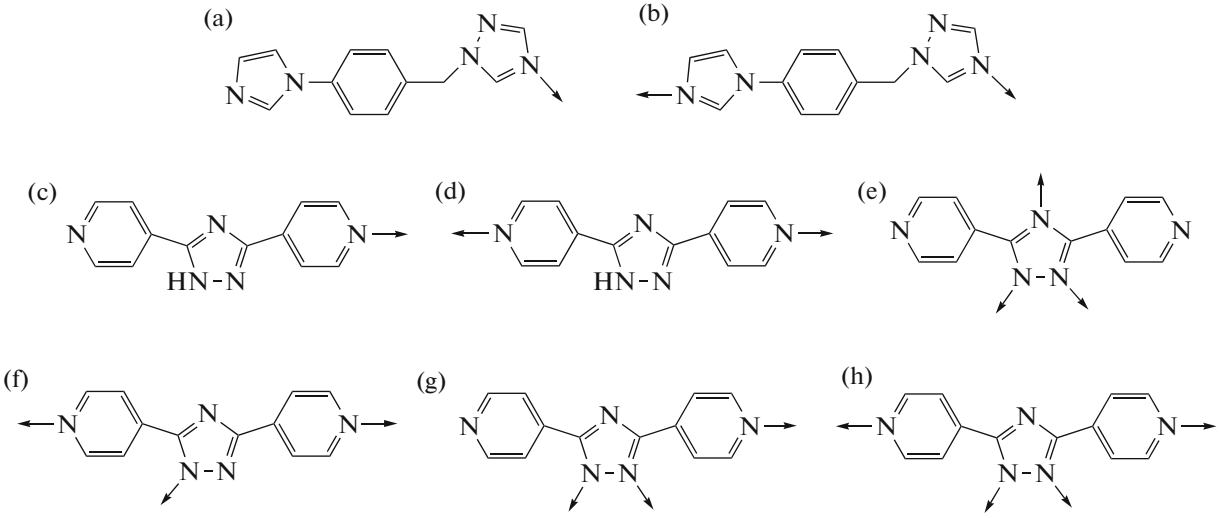

Scheme 1.

Herein, we demonstrate two new Cadmium(II)/Zinc(II) CPs constructed by aromatic dicarboxylate with flexible backbone (H_2Hmph = homophthalic acid) and Itmb/Bpt, namely: {[Cd(Hmph)(Otmb)] · H_2O}$_n$ (**I**) and [Zn(Hmph)(Bpt)$_2$]$_n$ (**II**). Their syntheses, crystal structures, thermal stabilities and fluorescent properties in the solid state were investigated.

EXPERIMENTAL

Materials and methods. All chemicals were purchased from commercial suppliers and used without further purification. The bulk products of both complexes were isolated, washed with distilled water, and then dried in air. The powder X-ray diffraction (PXRD) patterns of both complexes were recorded using a Bruker AXS D8 Advance diffractometer with monochromated CuK_α radiation. Elemental analyses for C, H, and N were measured on a Vario EL III elemental analyzer. The thermogravimetric (TG) analyses were carried out on a SII EXStar6000 TG/DTA6300 analyzer. Fluorescent properties of the solid samples were performed on an Aminco Bowman Series 2 luminescence spectrometer with xenon arc lamp.

Synthesis of I. A mixture of Cd(OAc)$_2$ · 2H_2O (53 mg, 0.20 mmol), H_2Hmph (18 mg, 0.10 mmol), Itmb (23 mg, 0.10 mmol), NaOH aqueous solution (0.5 M, 0.1 mL) and H_2O (6 mL) was sealed in a Teflon-lined stainless steel reactor, heated at 120°C for 3 days under autogenous pressure, and then cooled naturally to room temperature. The yield was 51% based on Cd(II). Colorless block crystals suitable for single crystal X-ray analysis were received.

For $C_{21}H_{19}N_5O_5Cd$

Anal. calcd., %	C, 47.25	H, 3.59	N, 13.12
Found, %	C, 47.23	H, 3.65	N, 13.09

Synthesis of II. Using Zn(OAc)$_2$ · 2H_2O (44 mg, 0.20 mmol), H_2Hmph (18 mg, 0.10 mmol), Bpt (45 mg, 0.20 mmol) and H_2O (6 mL) as the starting materials, colorless block crystals of complex **II** were received by the identical method as that for complex **I**. The yield was 43% based on Zn(II).

For $C_{33}H_{24}N_{10}O_4Zn$

Anal. calcd., %	C, 57.44	H, 3.51	N, 20.30
Found, %	C, 57.41	H, 3.55	N, 20.29

X-ray crystallography. Diffraction data for complexes **I**, **II** was recorded on a Bruker SMART APEX II CCD diffractometer equipped with graphite-monochromated MoK_α radiation (λ = 0.71073 Å) at room temperature. All non-hydrogen atoms were solved using SHELXS-97 program package by direct methods and refined with SHELXL-97 program package by full-matrix least-squares on F^2 [29, 30]. The hydrogen atoms of the dicarboxylate and 1,2,4-triazole ligands lay on the calculated positions refined isotropically with a riding model. The hydrogen atoms of the H_2O molecule were placed in a difference-Fourier map and refined by using geometrical restraints. The crystal data and structure refinement for complexes **I** and **II** are detailed in Table 1, the selected bond lengths and angles are shown in Table 2.

Supplementary material for structure **I** has been deposited with the Cambridge Crystallographic Data Centre (CIF files CCDC nos. 1842595 (**I**), 1842591 (**II**)); deposit@ccdc.cam.ac.uk or http://www.ccdc. cam.ac.uk).

Table 1. Crystallographic data and structure refinement for complex **I** and **II**

Parameter	Value	
Formula weight	533.81	689.99
Temperature, K	293(2)	296(2)
Crystal system	Triclinic	Triclinic
Space group	$P\bar{1}$	$P\bar{1}$
a, Å	8.699(3)	8.001(2)
b, Å	12.158(4)	8.015(2)
c, Å	12.277(4)	23.324(7)
α, deg	63.883(6)	86.976(8)
β, deg	77.446(7)	87.823(8)
γ, deg	73.800(7)	87.054(7)
Volume, Å^3; Z	1112.8(6); 2	1490.8(7); 2
ρ_{calcd}, mg/m^3	1.593	1.537
θ Range for data collection, deg	1.86–25.37	0.87–25.36
Reflections collected/unique	7164/4043	9547/5348
R_{int}	0.0211	0.0438
Goodness-of-fit on F^2	1.034	1.089
Final R indices ($I > 2\sigma(I)$)	$R_1 = 0.0251$, $wR_2 = 0.0607$	$R_1 = 0.0682$, $wR_2 = 0.2508$
R indices (all data)	$R_1 = 0.0280$, $wR_2 = 0.0624$	$R_1 = 0.0833$, $wR_2 = 0.2649$
Largest diff. peak and hole, e Å^{-3}	0.525 and –0.300	0.959 and –0.588

RESULTS AND DISCUSSION

Both complexes were synthesized by facile hydrothermal route. The higher reaction temperature and system pressure benefits the preparation of relevant single crystals, avoiding effectively the formation of precipitation in aqueous solution.

The asymmetric unit of complex **I** comprises one Cd^{2+} cation, one completely deprotonated Hmph ligand, one Itmb molecule and one unligated water, as shown in Fig. 1a. The unique Cd atom is seven-coordinated by five oxygen atoms from three symmetry related Hmph dianions and two nitrogen atoms from two Itmb molecules. All the Cd–O distances are in the range of 2.303(2)–2.505(2) Å, and the Cd–N distances are 2.252(2) and 2.374(2) Å, respectively. The neighbor Cd atoms are double bridged together by two μ_2-O bridges from $-CH_2COOH$ groups to generate a $[Cd_2O_8]$ dinuclear subunit (Fig. 1b), wherein the Cd···Cd distance is 4.0060(12) Å. The repeating dinuclear subunits are connected by μ_2 $Hmph^{2-}$ ligands to form a double-strand chain along a direction, with $-CH_2COOH$ groups in μ_3-η^2:η^1 mode and –COOH groups in μ_2-η^1:η^1 chelating mode. These adjacent 1D motifs are further bridged by the Itmb coligands to produce a 2D layer structure (Fig. 1c). And the Itmb molecule displays the coordination mode (Scheme 1b) [23]. The hydrogen-bonding interactions between free water molecules and $Hmph^{2-}$ ligands are observed in the 2D layer only. Some details of the hydrogen-bonding interactions are listed in Table 3. Furthermore, the ultimate 3D supramolecular structure is stabilized by significant π–π interactions between the phenyl rings of Itmb coligands with the centroid-centroid distances of 4.0231(10) Å (Figs. 1d, 1e).

The asymmetric unit of **II** comprises one Zn^{2+} cation, one completely deprotonated Hmph dianion and two Bpt molecules, as shown in Fig. 2a. The unique Zn atom displays a distorted tetrahedron geometry with the coordination sphere defined by two oxygen

Table 2. Selected bond distances and angles for **I** and **II***

Bond	*d*, Å	Bond	*d*, Å
		I	
Cd(1)–O(1)	2.422(2)	Cd(1)–O(2)	2.410(2)
Cd(1)–O(1)^{iii}	2.505(2)	Cd(1)–O(3)^{i}	2.481(2)
Cd(1)–O(4)^{i}	2.303(2)	Cd(1)–N(1)	2.252(2)
Cd(1)–N(5)^{ii}	2.374(2)		
		II	
Zn(1)–O(1)	1.925(4)	Zn(1)–O(3)^{i}	1.950(4)
Zn(1)–N(1)	2.029(5)	Zn(1)–N(6)	2.053(5)
Angle	ω, deg	Angle	ω, deg
		I	
O(1)Cd(1)O(3)^{i}	148.96(7)	O(1)Cd(1)O(1)^{iii}	71.24(8)
O(2)Cd(1)O(1)	52.98(7)	O(2)Cd(1)O(3)^{i}	135.12(7)
O(2)Cd(1)O(1)^{iii}	118.23(7)	O(3)^{i}Cd(1)O(1)^{iii}	82.56(7)
O(4)^{i}Cd(1)N(5)^{ii}	97.46(7)	O(4)^{i}Cd(1)O(2)	87.24(8)
O(4)^{i}Cd(1)O(1)	104.38(7)	O(4)^{i}Cd(1)O(3)^{i}	54.57(6)
O(4)^{i}Cd(1)O(1)^{iii}	82.44(7)	N(1)Cd(1)O(4)^{i}	152.61(7)
N(1)Cd(1)N(5)^{ii}	88.81(7)	N(1)Cd(1)O(2)	120.15(8)
N(1)Cd(1)O(1)	93.04(7)	N(1)Cd(1)O(3)^{i}	100.36(7)
N(1)Cd(1)O(1)^{iii}	83.43(7)	N(5)^{ii}Cd(1)O(2)	80.02(7)
N(5)^{ii}Cd(1)O(1)	125.95(7)	N(5)^{ii}Cd(1)O(3)^{i}	82.52(7)
N(5)^{ii}Cd(1)O(1)^{iii}	161.65(7)		
		II	
O(1)Zn(1)O(3)^{i}	116.5(2)	O(1)Zn(1)N(1)	106.0(2)
O(3)^{i}Zn(1)N(1)	107.0(2)	O(1)Zn(1)N(6)	125.77(19)
O(3)^{i}Zn(1)N(6)	94.67(19)	N(1)Zn(1)N(6)	105.27(19)

* Symmetry transformations used to generate equivalent atoms: ^{i} $x-1, y, z$; ^{ii} $x, y+1, z-1$; ^{iii} $-x, -y, -z$ (**I**). ^{i} $x-1, y, z$ (**II**).

Table 3. Geometric parameters of hydrogen bonds for **I** and **II***

	Distance, Å			Angle DHA, deg
D–H···A	D–H	H···A	D···A	
		I		
O(5*w*)–H(1*w*)···O(2)^{iv}	0.85	2.33	3.181(4)	179.7
O(5*w*)–H(2*w*)···O(3)^{iv}	0.85	2.15	2.983(4)	166.4
		II		
N(4)–H(4N)···O(4)^{ii}	0.86	1.93	2.779(7)	170.5
N(8)–H(8N)···O(2)^{iii}	0.86	1.95	2.752(7)	155.4

* Symmetry codes: ^{iv} $-x+1, -y+1, -z$ (**I**). ^{ii} $x-1, y-1, z$; ^{iii} $-x+2, -y+1, -z$ (**II**).

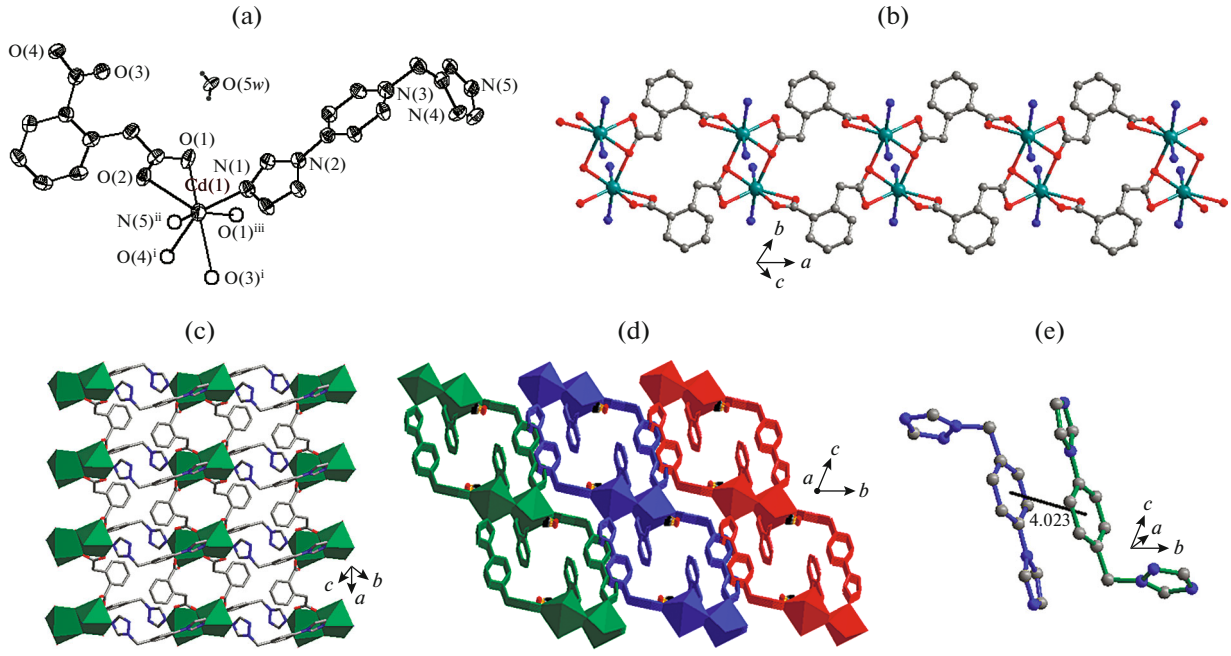

Fig. 1. View of the coordination environment of Cd(II) in **I** (a); view of the double-strand chain constructed by $[Cd_2O_8]$ dinuclear subunits (b); view of the 2D sheet structure (c); view of the 3D packing of complex **I** (d); view of the π–π interactions between the phenyl rings of Itmb coligands (e). Symmetry codes: [i] $-1 + x, y, z$; [ii] $x, y + 1, z - 1$; [iii] $-x, -y, -z$; displacement ellipsoids are drawn at the 50% probability level and all hydrogen atoms of carbon atoms are omitted for clarity.

atoms from the $-COO^-$ and $-CH_2COO^-$ groups belonging to two symmetry related $Hmph^{2-}$, and two N atoms from two Bpt molecules. The Zn–O bond lengths are 1.925(4) and 1.950(4) Å, while the Zn–N bond lengths are 2.029(5) and 2.053(5) Å, respectively. The neighbor tetrahedra are connected by μ_2 Hmph dianions to form a zigzag metal-organic chain along *a* direction (Fig. 2b). And the Bpt molecules act only as pendent arms since they adopt the same coordination mode as observed in previously reported compound $[Ni(Hb)_2(Bpt)_2(H_2O)]_n$ (Scheme 1c, HHb = *p*-hydroxybenzoate acid) [24]. The adjacent 1D motifs are bridged by the hydrogen-bonding interactions between N(8) and O(2) to generate one double-strand chain motif, which is further extended to produce a layer structure lying in the *ab* plane via the hydrogen-bonding interactions between N(4) and O(4) (Figs. 2c, 2d). And the data of hydrogen-bonding interactions for **II** are listed in Table 3. Furthermore, individual layers are stacked to create the ultimate 3D supramolecular structure through significant π–π interactions between the triazolyl rings of Bpt ligands with the centroid-centroid distances of 3.964 Å (Fig. 2e).

Before the fundamental properties were investigated, it is necessary to confirm the phase purities of the as-synthesized samples by PXRD measurements. The positions of major peaks for both CPs match well with those of simulated PXRD patterns, indicating their reasonable purities.

To investigate the thermal stabilities of complexes **I** and **II**, TG experiments were performed by heating the bulk products with a heating rate of 10°C min^{-1} under nitrogen atmosphere (Fig. 3). Complex **I** undergoes the initial weight-loss process of 4.64% before 80°C. This is higher than the calculated value corresponding to the release of one lattice water molecule (3.37%), since about half disordered water molecule has been squeezed out by PLATON program. And the decomposition of organic ligands leads to the succeeding weight loss between 275 and 772°C. The final residue is assigned to CdO phase (found 23.81%, calcd. 24.06%). Complex **II** can bear high temperature and then collapse gradually from 315 to 596°C. The remnant weighing 14.14% of the total sample may be the mixture of ZnO (calcd. 11.79%) and unburned carbon [31].

The fluorescent properties of the free organic ligands, complexes **I** and **II** in the solid state were detected at room temperature, as illustrated in Fig. 4. It is observed that the free ligands have unremarkable emissions with the maximum at 452 nm (λ_{ex} = 390 nm) for H_2Hmph and 478 nm (λ_{ex} = 434 nm) for

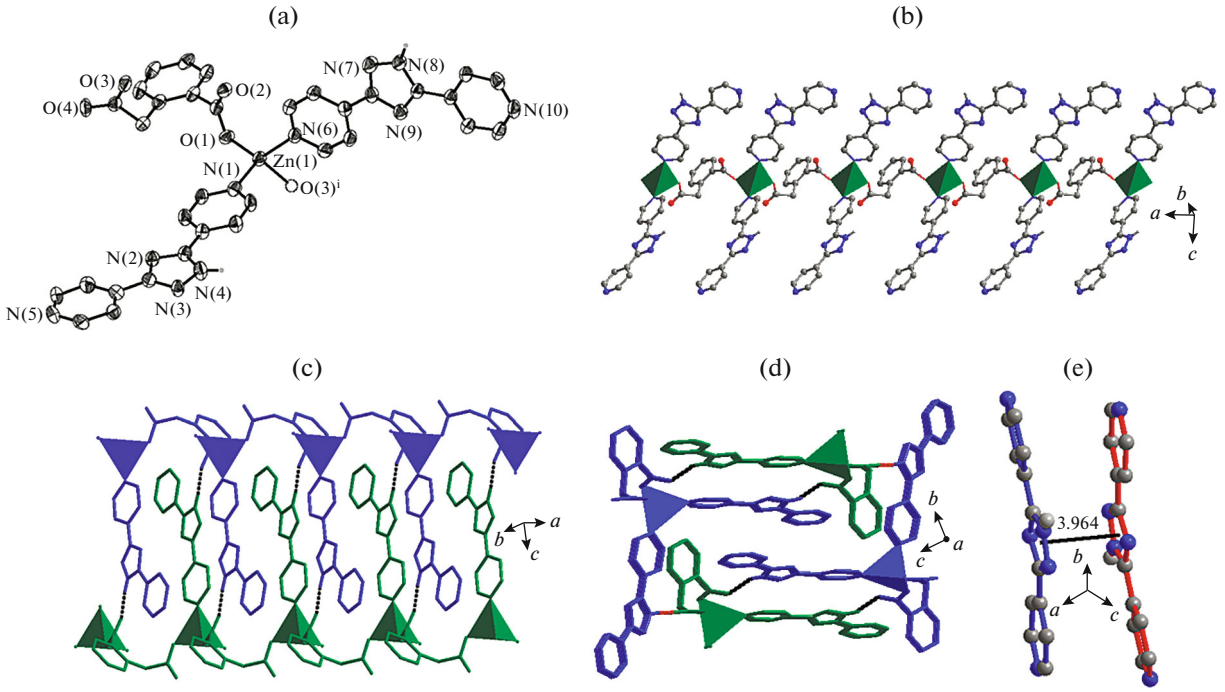

Fig. 2. View of the coordination environment of Zn(II) in **II** (a); view of a zigzag Zn-carboxylate chain along *a* direction with the bpt molecules acting as arms (b); view of the double-strand chain motif bridged by H-bond interactions (c); view of the layer structure extended via H-bond interactions (d); view of the π–π interactions between the triazolyl rings of Bpt ligands (e). Symmetry codes: ^{i} −1 + *x*, *y*, *z*; displacement ellipsoids are drawn at the 50% probability level and all hydrogen atoms of carbon atoms are omitted for clarity.

Bpt, while the Itmb ligand exhibits broad peaks with maxima at 416 nm (λ_{ex} = 350 nm). And complexes **I** and **II** display similar emission spectra with the maximum at 373 nm (λ_{ex} = 303 nm) and 363 nm (λ_{ex} = 274 nm), respectively. Considering the nature of metal centers with d^{10} configuration and similar emission spectra of the related complexes, they can probably be attributed to the ligand localized emission originating

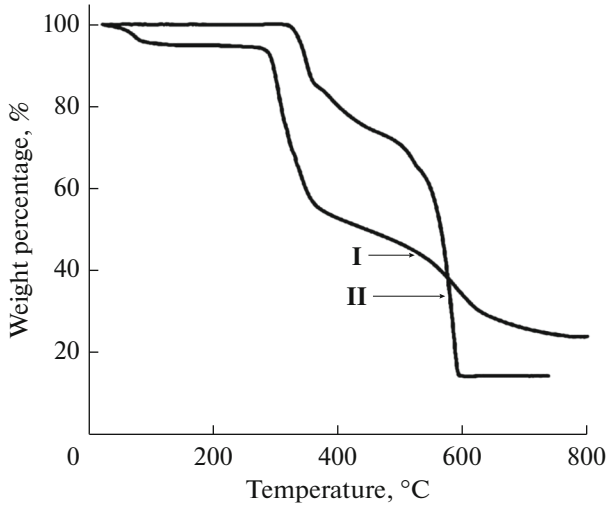

Fig. 3. The TG curves for complexes **I** and **II**.

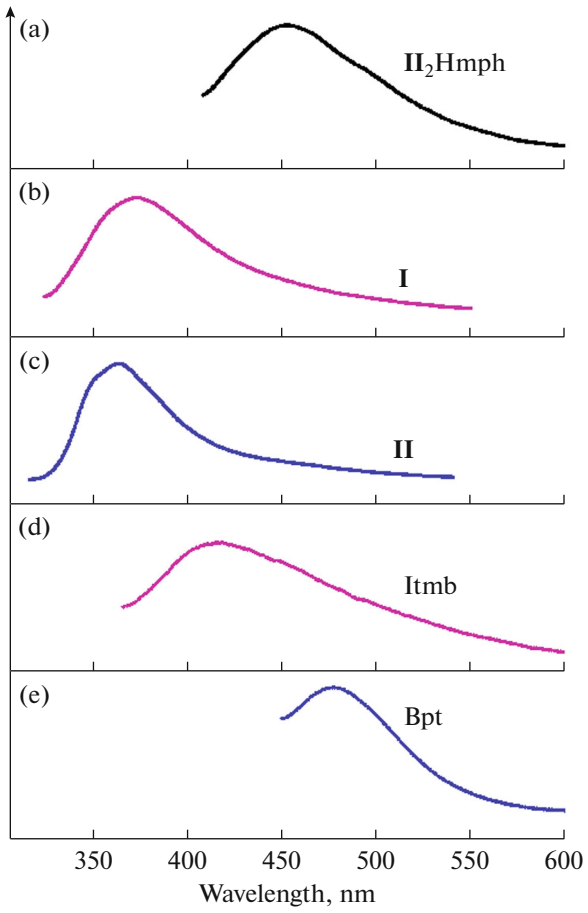

Fig. 4. The solid-state emission spectra of the free organic ligands, complexes **I** and **II**.

from the cooperation of H_2Hmph ligand and 1,2,4-triazole derivatives. In comparison with the powder precursors, those of two CPs show significant blue-shift, which are presumably owing to the coordination interactions of the $Hmph^{2-}$ ligand and 1,2,4-triazole derivatives to the central metal ions [32, 33].

In conclusion, we have realized two CPs by using Zn(II)/Cd(II) acetate, homophthalic acid, 1-(imidazo-1-yl)-4-(1,2,4-triazole-1-ylmethyl)benzene or 3,5-bis(4-pyridyl)-1,2,4-triazole as starting materials. Both complexes possess metal-carboxylate chain structure. Cd-carboxylate chains in complex **I** are linked to 2D layer structure by Itmb coligands, while Zn-carboxylate chains in complex **II** can not be extended because the Bpt coligands can only act as arms. In addition, complex **II** shows higher thermal stability than complex **I** since their framework start to collapse at 315 and 275°C, respectively. And presumably owing to the coordination interactions, the fluorescent emission spectra of both CPs show significant blue-shift compared with those of the free ligands.

ACKNOWLEDGMENTS

This work was supported by the National Natural Science Foundation of China (no. 21571093) and Colleges and Universities Key Scientific Research Project of Henan Province (no. 18B150016).

REFERENCES

1. Hendon, C.H., Rieth, A.J., Korzyński, M.D., et al., *ACS Cent. Sci.*, 2017, vol. 3, p. 554.
2. Li, J.R., Sculley, J., and Zhou, H.C., *Chem. Rev.*, 2012, vol. 112, p. 869.
3. Liu, T.F., Lu, J., and Cao, R., *CrystEngComm*, 2010, vol. 12, p. 660.
4. Wang, W.B., Wang, R.Y., Liu, L.N., et al., *Cryst. Growth Des.*, 2018, vol. 18, p. 3449.
5. Badiane, A., Freslon, S., Daiguebonne, C., et al., *Inorg. Chem.*, 2018, vol. 57, p. 3399.
6. Bakkali, H.E., Choquesillo-Lazarte, D., Domínguez-Martín, A., et al., *Cryst. Growth Des.*, 2014, vol. 14, p. 889.
7. Yin, Z., Zhou, Y.L., Zeng, M.H., et al., *Dalton Trans.*, 2015, vol. 44, p. 5258.
8. Tanasaro, T., Adpakpang, K., Ittisanronnachai, S., et al., *Cryst. Growth Des.*, 2018, vol. 18, p. 16.
9. Bae, Y., Mulfort, K.L., Frost, H., et al., *Langmuir*, 2008, vol. 24, p. 8592.
10. Xin, L.Y., Liu, G.Z., Li, X.L., et al., *Cryst. Growth Des.*, 2012, vol. 12, p. 147.
11. Liu, G.Z., Li, X.L., Xin, L.Y., et al., *CrystEngComm*, 2012, vol. 14, p. 5315.
12. Li, G.L., Liu, G.Z., Ma, L.F., et al., *Chem. Commun.*, 2014, vol. 50, p. 2615.
13. Das, D. and Biradha, K., *Cryst. Growth Des.*, 2018, vol. 18, p. 3683.
14. Boer, S.A. and Turner, D.R., *Cryst. Growth Des.*, 2016, vol. 16, p. 6294.
15. Ju, F.Y., Li, Y.P., Li, G.L., et al., *Chin. J. Struct. Chem.*, 2016, vol. 35, p. 404.
16. Li, X.L., Liu, G.Z., Xin, L.Y., et al., *J. Solid State Chem.*, 2017, vol. 246, p. 252.
17. Wang, Y.F., Wei, J.J., and Zhai, X.H., *Russ. J. Coord. Chem.*, 2018, vol. 44, p. 183. https://doi.org/10.1134/S1070328418030065
18. Du, M., Jiang, X.J., and Zhao, X.J., *Inorg. Chem.*, 2007, vol. 46, p. 3984.
19. Xie, X.F., Chen, S.P., Xia, Z.Q., et al., *Polyhedron*, 2009, vol. 28, p. 679.
20. Park, Y.J., Ryu, J.Y., Hwang, S., et al., *Inorg. Chem.*, 2017, vol. 56, p. 14060.
21. Zhuang, G.M., Li, X.B., and Gao, E.Q., *Inorg. Chem. Commun.*, 2014, vol. 47, p. 134.
22. Yu, Y., Ma, H.Y., Pang, H.J., et al., *New J. Chem.*, 2014, vol. 38, p. 1271.
23. Xin, L.Y., Li, X.L., and Liu, G.Z., *Kristallogr. NCS*, 2016, vol. 231, p. 1215.
24. Wu, M.C., Li, H.Y., and Huang, F.P., *J. Chem. Res.*, 2013, vol. 37, p. 136.

25. Huang, F.P., Bian, H.D., Yu, Q., et al., *CrystEngComm*, 2011, vol. 13, p. 6538.
26. Zhang, J.P., Lin, Y.Y., Huang, X.C., et al., *Cryst. Growth Des.*, 2006, vol. 6, p. 519.
27. Li, B.Y., Jin, D., Ma, B.H., et al., *Eur. J. Inorg. Chem.*, 2011, vol. 2011, p. 35.
28. Jin, X.M., Xu, Q.F., Zhou, Q., et al., *Chin. J. Inorg. Chem.*, 2009, vol. 25, p. 539.
29. Sheldrick, G.M., *SHELXS-97, Program for X-ray Crystal Structure Determination*, Göttingen: Univ. of Göttingen, 1997.
30. Sheldrick, G.M., *Program for X-ray Crystal Structure Refinement*, Göttingen: Univ. of Göttingen, 1997.
31. Li, Y.P., Ju, F.Y., Li, G.L., et al., *Russ. J. Coord. Chem.*, 2018, vol. 44, p. 214. https://doi.org/10.1134/S1070328418030028
32. Bai, H.Y., Ma, J.F., Yang, J., et al., *Cryst. Growth Des.*, 2010, vol. 10, p. 1946.
33. Chang, X.H., Zhao, Y., Feng, X., et al., *Polyhedron*, 2014, vol. 83, p. 159.